Author Manuscript

Title: Single-Step Synthesis of Atropisomers with Vicinal C–C and C–N Diaxes by Cobalt-Catalyzed Atroposelective C–H Annulation

Authors: Bing-Jie Wang; Guo-Xiong Xu; Zong-Wei Huang; Xu Wu; Xin Hong; Qi-Jun Yao; Bing-Feng Shi, Prof.

RESEARCH ARTICLE

Single-Step Synthesis of Atropisomers with Vicinal C–C and C–N Diaxes by Cobalt-Catalyzed Atroposelective C–H Annulation

Bing-Jie Wang,[a] Guo-Xiong Xu,[a] Zong-Wei Huang,[c] Xu Wu,[a] Xin Hong,[a],* Qi-Jun Yao,[a],* and Bing-Feng Shi[a,b]*

[a] B.-J. Wang, G.-C. Xu, X. Wu, Prof. Dr. X. Hong, Dr. Q.-J. Yao, Prof. Dr. B.-F. Shi
Center of Chemistry for Frontier Technologies, Department of Chemistry, Zhejiang University, Hangzhou 310027, China
Email: hxchem@zju.edu.cn; 3110000156@zju.edu.cn; bfshi@zju.edu.cn
Homepage: http://mypage.zju.edu.cn/en/bfshi/
[b] Prof. Dr. B.-F. Shi
Green Catalysis Center, College of Chemistry, Zhengzhou University, Zhengzhou 450001, China
[c] Z.-W. Huang
Department of Chemistry, University of Michigan, Ann Arbor, Michigan 48109, United States

Abstract: The atroposelective synthesis of atropisomers with vicinal diaxes remains rare and challenging, due to the steric influence between the two axes and their unique topology. Herein, we disclose a single-step construction of atropisomers with vicinal C–C and C–N chiral diaxes by cyclopentadiene (Cp)-free cobalt-catalyzed intramolecular atroposelective C-H annulation, providing the desired diaxial atropisomers of unique structures with decent stereocontrols of both axes (up to >99% ee and 70:1 dr). The optically pure products bearing fluorophores show circular polarized luminescence (CPL) properties, being candidate materials for potential CPL applications. Atropisomerization experiments and density function theory (DFT) calculations are conducted to study the rotational barriers and rotation pathways of the diaxes.

Introduction

The past decades have witnessed the emergence of transition metal-catalyzed enantioselective C–H activation strategy to access complex chiral molecules in a step- and atom-economical manner.[1] In particular, enantioselective C–H functionalization has provided an efficient strategy for the synthesis of atropisomers, an important class of enantiomers arising from restricted rotation around a single bond.[2] Despite remarkable advances have been achieved, the majority of these studies focus on the enantioselective synthesis of atropisomers with a single axis and only a few examples on the synthesis of atropisomers with isolated double or multiple axes have been reported.[3,4] The enantioselective preparation of atropisomers with vicinal chiral diaxes remains a formidable challenge due to the steric influence between the two axes and their unique topology, and of which the successful examples are extremely rare (Figure 1a).[5] In 2018, the group of Wencel-Delord and Colobert developed a concise synthesis of chiral o-terphenyls by chiral sulfoxide-directed palladium-catalyzed diastereoselective C–H arylation.[6] Recently, Zhou and coworkers reported the synthesis of atropisomeric o-terphenyls with vicinal diaxes via atroposelective Catellani reaction using palladium/chiral norbornene cooperative catalysis (Figure 1b).[7] Although these elegant studies showcase the concept of enantioselective C–H activation strategy in the synthesis of atropisomers with vicinal diaxes, the reactions were limited to the preparation of chiral o-terphenyls via the formation of C–C axis, and the use of expensive palladium catalyst and

chiral ligand/auxiliary. The construction of atropisomers bearing vicinal diaxes with more labile C–N axis has not been reported yet.

On the basis of our recent interests in the enantioselective synthesis of atropisomeric compounds, such as biaryls, anilides, and styrenes via C-H activation strategy,[8] we became interested in the synthesis of more challenging atropisomers with vicinal C–C and C–N chiral diaxes via enantioselective C–H activation. We designed a type of benzamides **1** bearing an 8-aminoquinoline directing group (DG)[9] and an alkyne moiety tethered at the *meta*-position. We reasoned that the judicious choice of metal catalyst and chiral ligand might enable the enantioselective intramolecular C–H annulation (Figure 1c). In the working hypothesis, C–H metalation would lead to the formation of the cyclometalated intermediate **Int-1**, which might undergo a stereo-determining migratory insertion with the assistance of the ligated chiral ligand (**L***) to afford axially chiral **Int-2** with a chiral C–C axis. Subsequent C–N reductive elimination of **Int-2** would construct the isoquinolinone ring and fix the C–N axis of the C(O)–N-quinoline. Although it is strategically feasible, we are aware that the proposed protocol would face several challenges. First, the cleavage of the sterically encumbered *ortho*-C–H bond with a *meta*-substitution to form **Int-1** is a prerequisite to enable the subsequent intramolecular insertion while it is known that C–H metalation is generally sterically sensitive and C–H bonds with 1,3-disubstitutions are generally less reactive. We reasoned that cobalt catalyst might be a suitable catalyst due to the small ionic radius.[10] In addition, the *O*-tethered alkyne side chain might assist the cleavage of the C–H bonds.[11] Second, based on the working hypothesis, both of the migratory insertion (**Int-1→Int-2**) and C–N reductive elimination (**Int-2→2**) steps should be stereoselective to control the formation of axially chiral C–C and C–N diaxes. Therefore, the judicious choice of a well-designed chiral ligand (**L***) that coordinates to the metal catalyst during the whole process of the catalysis to provide a long-lasting chiral environment for stereoinduction is essential to the success of the protocol. Nevertheless, we were encouraged by our recent work on cobalt-catalyzed desymmetrizing C–H functionalization of diarylphosphinamides with salicyloxazoline (Salox) as the chiral ligand, in which the Salox ligand enabled the *in situ* oxidation of cobalt(II) salt to generate the active octahedral cobalt(III) catalyst and acted as a permanent bidentate ligand during the whole process.[12] Third, compared to the well-established C–C atropisomers, the C–N atropisomeric axes generally bear lower configurational stability, rendering their enantioselective construction more challenging.[13] Especially, the formation of

labile C–N axis might be significantly affected by the steric interactions between the preformed vicinal C–C axis in **Int-2**.

Herein, we disclose our strategy to address these challenges and report the enantioselective synthesis of atropisomers with vicinal C–C and C–N chiral diaxes by cyclopentadiene (Cp) free cobalt-catalyzed intramolecular atroposelective C–H annulation.[14] Cheap and commercially available cobalt(II) salt was used as precatalyst and simple Salox was used as chiral ligand, providing the diaxial atropisomers of unique structures with decent stereocontrols of both axes (up to >99% ee and 70:1 dr). The optically pure products bearing fluorophores show circular polarized luminescence (CPL) properties, being candidate materials for potential CPL applications. Atropisomerization experiments and DFT calculations are conducted to study the rotational barriers and rotation pathways of the diaxes.
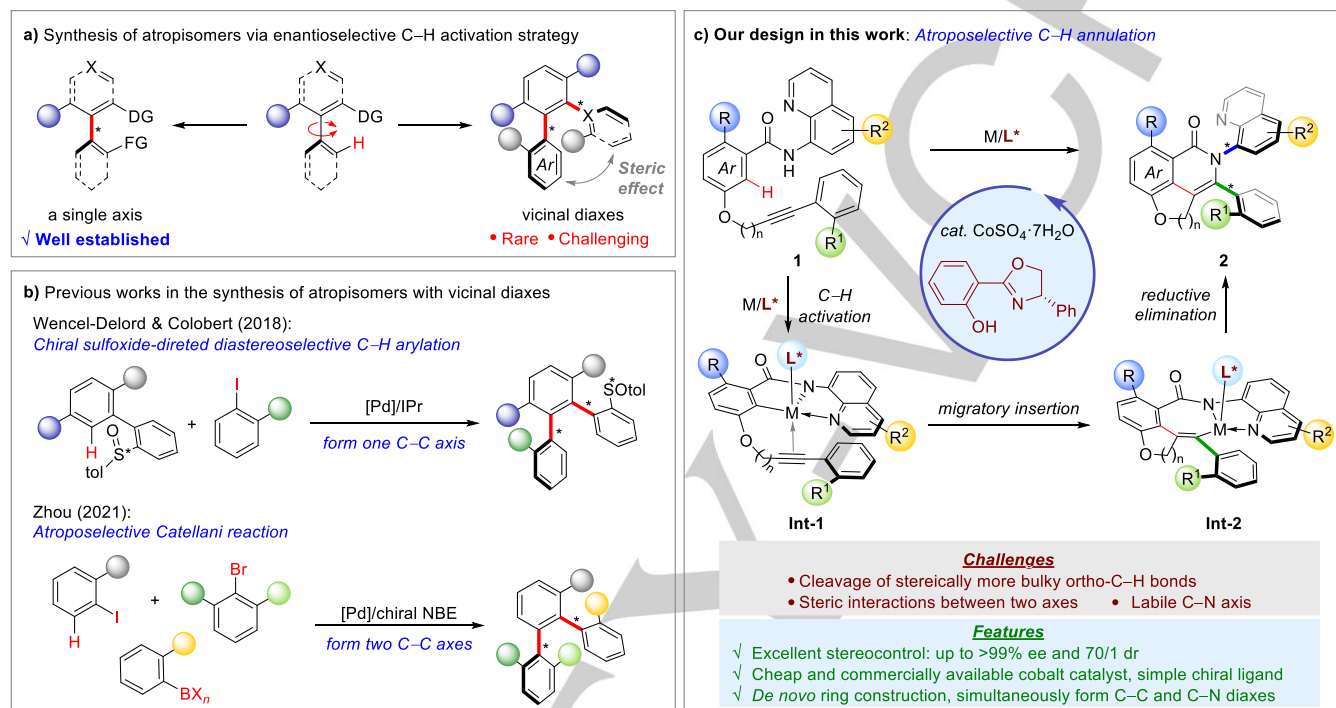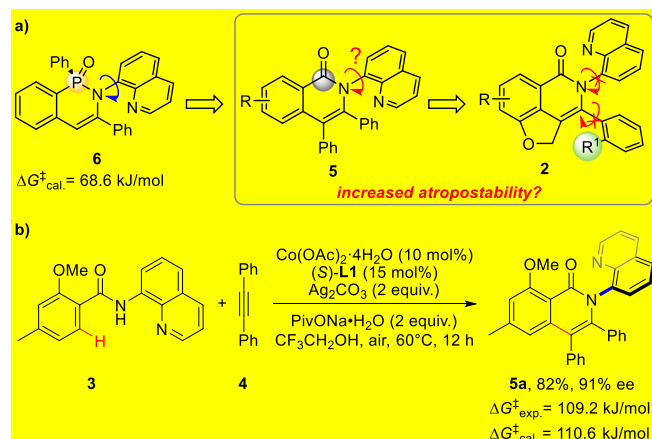

Figure 1. Construction of atropisomers with vicinal chiral diaxes via atroposelective C-H activation.

Results and Discussion

Initial Researches. We commenced our study by first investigating the possibility of the construction of chiral C-N axis. Our group recently reported the desymmetrizing C–H functionalization of diarylphosphinamides to prepare P-stereogenic chirality.[12] ^{1}H NMR spectrum of the product **6** showed two sets of peaks arisen from a pair of atropisomers of C–N axis at room temperature; but at 100°C, this phenomenon could not be seen, indicating an energy barrier for the C–N axis that could not be ignored ($\Delta G^{\ddagger}_{cal.}$ = 68.8 kJ/mol). We anticipated that the replacement of the chiral phosphine oxide moiety with a carbonyl would cause a significant increased atropostablility, offering possibilities for the construction of chiral C–N axis (Figure 2a).

To explore this idea, the intermolecular C–H annulation of benzamide **3** with dipenylacetylene **4** was conducted in trifluoroethanol catalyzed by Co(OAc)$_2$·4H$_2$O (10 mol%) and Salox (*S*)-**L1** (15 mol%) (Figure 2b).[15] As expected, the desired product **5a** was detected, and much to our surprise, isolated in decent yield and high enantioselectivity (82%, 91% ee). Then an atropisomerization experiment of **5a** was done in isopropanol at 75°C, revealing an energy barrier of 109.2 kJ/mol for the atropisomerization of C–N axis ($\Delta G^{\ddagger}_{cal.}$ = 110.6 kJ/mol). By Erying equation, the racemization half-life of **5a** was calculated as 8 days at 25°C (See supporting information for details). Based on these inspiring results, we reasoned that the introduction of an *ortho*-substituent (R^1) to the aryl at 3-position would not only lead to the formation of a new chiral C–C axis but also render the vicinal C–N axis more sterically hindered (Figure 2a), which might offer the opportunity to simultaneously construct C–C and C–N chiral diaxes.

Figure 2. a) Rational Design. b) Exploration of Intermolecular Atroposelective C–H Annulation.

Optimizing Reaction Conditions. With the feasibility of enantioselective construction of C–N atropisomer verified, we then commenced to investigate our hypothesis using the well-designed benzamide **1a** as the model substrate. To our delight, **1a** reacted smoothly using Co(OAc)$_2$·4H$_2$O (10 mol%) as precatalyst and Salox (S)-**L1** (20 mol%) as the chiral ligand, giving the expected intramolecular C–H annulated product **2a** in high yield with noticeable stereocontrols (Table 1, entry 1, 98% yield, 93% ee and 4.8/1 dr). The screening of cobalt(II) salts and solvents revealed that CoSO$_4$·7H$_2$O gave better dr value (entry 3, 6.4/1 dr) and n-propanol was the optimal solvent (entries 4-7). Since the atropostability is sensitive to temperature, we then investigate the reaction temperature. When the reaction was conducted at 50 °C, the yield and the enantioselectivity of the major diastereomer remained high (95%, 96% ee) with significantly enhanced diastereoselelctivity (entry 8, 23/1 dr). No better results were obtained when the temperatures were further reduced (entries 9 and 10). Next, a series of chiral Salox ligands were tested. Salox ligand with a methoxy substituent at the para-position of phenolic hydroxyl (**L2**) led to reduced yield and stereocontrol (entry 11). Salox **L3** with t-butyl at ortho-position of phenol moiety was detrimental to the reaction (entry 12). An isopropyl (**L5**) or two phenyls (**L4**) on the oxazoline moiety dramatically reduced the enantioselectivity (entries 13 and 14). Generally, Salox ligands bearing a phenyl group attached to the oxazoine gave high enantioselectivity that comparable to **L1**, albeit with lower yield or slightly lower dr (Table S6, **L6**, **L7**, and **L15-L19**). The comparable enantiocontrol could be attributed to the π-π interaction between the phenyl ring on the oxazoline of **L1** and the quinoline moiety of **1a** (see cobaltacycle intermediate **QI** in the supporting information for details).[16] Mn(OAc)$_3$·2H$_2$O, an efficient oxidant first used by Daugulis and co-workers in cobalt-catalyzed C–H annulation reactions,[15] was found to be the optimal oxidant (see Table S4 for details). PivONa was the optimal base to promote the C–H activation step (see Table S5 for details).[11]

Scope of Substrates. With the optimized conditions established, the scope of the protocol was then explored (Table 2). Replacing R^1 with substituents of different sizes, such as methyl, ethyl, isopropyl, and chloro, did not detract from the good yields and ee values (**2a-2d**). Surprisingly, ortho-trifluoromethyl substituted benzamide **1e** gave relatively lower enantioselectivity and diastereoselectivity. As expected, **2f** with only one C–N chiral axis was obtained in high yield with good enantioselectivity (90%, 89% ee). Benzamides with disubstituted terminal aryl and naphthyl also gave the desired products in excellent enantioselectivities and good diastereoselectivities (**2g-2i**, 96% to 98% ee, 8/1 to 14/1 dr). A variety of substituents (R = OMe, Cl, F, Br, aryls) at the C2-position of benzamides and on quinoline (R^2 = Cl, Br, OMe, phenyl) were well tolerated, giving the products with good to excellent enantio- and diastereoselectivity ((**2j-2s**) 89 to >99% ee major and 12/1 to 56/1 dr), although **2j** with a methoxy group was obtained in a lower yield of 24%. Different linkers were then examined. Benzamide **1t** with a gem-dimethyl group reacted well, giving **2t** in 86% yield with excellent enantioselectivity (>99% ee major, 99% ee minor), albeit almost no diastereoselectivity (1.2/1 dr). Benzamide **1u** with a longer chain significantly reduced the stereo-control (**2u**, 66% ee major, 80% ee minor and 1.4/1 dr). Notably, heterocyclic and olefinic C–H bonds were both suitable for this reaction, showing excellent enantiocontrols (**2v** and **2w**, >99% ee for both diastereomers). Unfortunately, no desired product was obtained when benzamide **1x** with sulfonamide moiety was used. The absolute configurations of products **2a**, **2d** and **2m** were unambiguously determined by X-ray crystallographic analysis as (3S,4R), and those of the others were assigned by analogy.[16]

Author Manuscript

Table 1. Reaction optimization.[a]

entry	[Co]	solvent	T (°C)	ligand	yield (%)[b]	ee major (%)[c,d]	ee minor (%)[c,d]	dr[d]
1	Co(OAc)$_2$·4H$_2$O	^{t}BuOH	60	**L1**	98	93	19	4.8/1
2	Co(acac)$_2$·xH$_2$O	^{t}BuOH	60	**L1**	95	81	15	3.3/1
3	CoSO$_4$·7H$_2$O	^{t}BuOH	60	**L1**	82	93	28	6.4/1
4	CoSO$_4$·7H$_2$O	EtOH	60	**L1**	71	93	27	5.2/1
5	CoSO$_4$·7H$_2$O	TFE	60	**L1**	29	96	92	2.1/1
6	CoSO$_4$·7H$_2$O	Et$_2$O	60	**L1**	49	96	-4	4.7/1
7	CoSO$_4$·7H$_2$O	^{n}PrOH	60	**L1**	99	96	20	6.9/1
8	**CoSO$_4$·7H$_2$O**	**^{n}PrOH**	**50**	**L1**	**95**	**96**	**95**	**23/1**
9	CoSO$_4$·7H$_2$O	^{n}PrOH	40	**L1**	93	93	87	17/1
10	CoSO$_4$·7H$_2$O	^{n}PrOH	30	**L1**	86	97	92	22/1
11	CoSO$_4$·7H$_2$O	^{n}PrOH	50	**L2**	84	67	78	13/1
12	CoSO$_4$·7H$_2$O	^{n}PrOH	50	**L3**	0	-	-	-
13	CoSO$_4$·7H$_2$O	^{n}PrOH	50	**L4**	45	78	77	11/1
14	CoSO$_4$·7H$_2$O	^{n}PrOH	50	**L5**	53	53	60	16/1

[a] Reaction conditions: **1a** (0.05 mmol), [Co] (10 mol%), Mn(OAc)$_3$·2H$_2$O (0.05 mmol), PivONa·2H$_2$O (0.1 mmol), ligand (20 mol%) in 1 mL ^{n}PrOH at 50°C under air for 24 h. [b] Isolated yield are provided. [c] Ee major and ee minor are the enantiomer excess of the major and minor diastereomers respectively. [d] The ee and dr were determined based on HPLC analysis. The dr values from HPLC and ^{1}H NMR matched well. TFE = trifluoroethanol. Ee = enantiomeric excess. Dr = diastereo ratio.
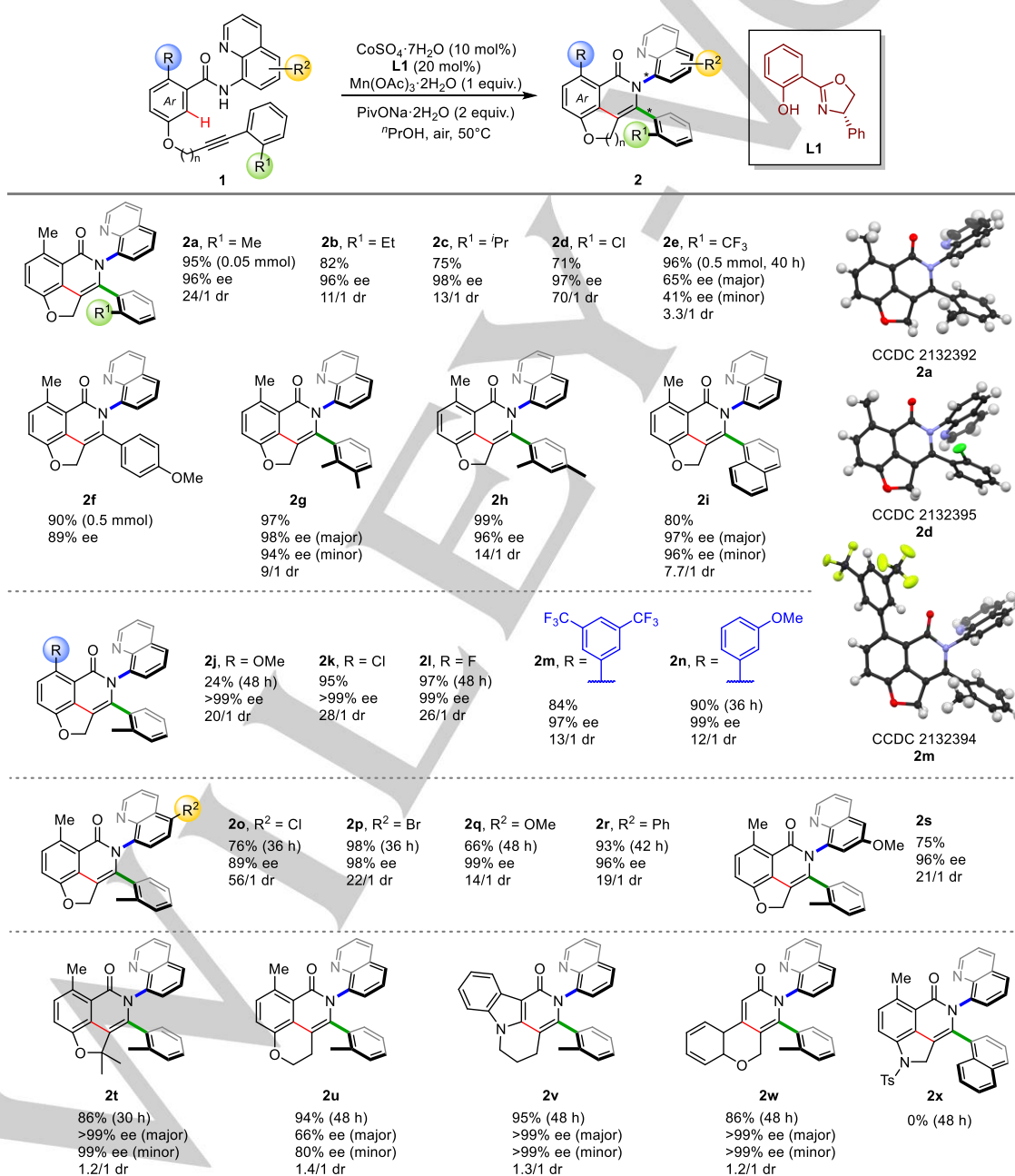
3

Gram-Scale Synthesis. To demonstrate the synthetic applicability, a gram-scale reaction was conducted, providing product **2a** without noticeable erosion of both yield and stereoselectivity (Scheme 1). A further purification by simple trituration of the crystals of **2a** in a mixture of acetone and diethyl ether gave **2a** with very high optical purity with minimal loss (1.231g, 76% overall yield, >99.9% ee, >100/1 dr).

Chiroptical Properties of Products. Since different aryls could be attached to the C2 position of benzamides, we wondered if a large conjugated aryl would introduce fluorescence properties to the molecules. **2y** and **2z** bearing a triphenylamine and a dibenzofuran moiety were synthesized on a decigram-scale and recrystallized to give higher optical purity (**2y**, 95% ee major, 50/1 dr; **2z**, 95% ee major, 37/1 dr). Intrigued by the bright fluorescence

of products **2y** and **2z**, we set about studying their (chir)optical properties by UV-visible spectra, fluorescence spectra, electronic circular dichroism (ECD), circularly polarized luminescence (CPL), and photo luminescence quantum yield (PLQY) measurements. The absorption maxima of **2y** is slightly red-shifted compared to those of **2z**. Their emissions peak at 475 nm (**2y**) and 438 nm (**2z**) (Figure 3a). The ECD and CPL spectra of **2y** and **2z** as well as their enantiomers **2y-ent** and **2z-ent** exhibit as decent mirror images (Figure S1, S2 and Figure 3b). Both **2y** and **2z** are CPL-active whose dissymmetry factors $|g_{lum}|$ are about 5×10^{-4} and 7×10^{-4} around the emission maxima respectively, comparable to those of reported organic small molecule CPL emitters.[17] Combined with PLQYs of 0.29 (**2y**) and 0.09 (**2z**), they could be candidate materials for potential CPL applications.

Table 2. Scope of the cobalt-catalyzed intramolecular atroposelective C–H annulation.[a]

2a, R¹ = Me
95% (0.05 mmol)
96% ee
24/1 dr

2b, R¹ = Et
82%
96% ee
11/1 dr

2c, R¹ = ⁱPr
75%
98% ee
13/1 dr

2d, R¹ = Cl
71%
97% ee
70/1 dr

2e, R¹ = CF₃
96% (0.5 mmol, 40 h)
65% ee (major)
41% ee (minor)
3.3/1 dr

CCDC 2132392
2a

2f
90% (0.5 mmol)
89% ee

2g
97%
98% ee (major)
94% ee (minor)
9/1 dr

2h
99%
96% ee
14/1 dr

2i
80%
97% ee (major)
96% ee (minor)
7.7/1 dr

CCDC 2132395
2d

2j, R = OMe
24% (48 h)
>99% ee
20/1 dr

2k, R = Cl
95%
>99% ee
28/1 dr

2l, R = F
97% (48 h)
99% ee
26/1 dr

2m, R =
84%
97% ee
13/1 dr

2n, R =
90% (36 h)
99% ee
12/1 dr

CCDC 2132394
2m

2o, R² = Cl
76% (36 h)
89% ee
56/1 dr

2p, R² = Br
98% (36 h)
98% ee
22/1 dr

2q, R² = OMe
66% (48 h)
99% ee
14/1 dr

2r, R² = Ph
93% (42 h)
96% ee
19/1 dr

2s
75%
96% ee
21/1 dr

2t
86% (30 h)
>99% ee (major)
99% ee (minor)
1.2/1 dr

2u
94% (48 h)
66% ee (major)
80% ee (minor)
1.4/1 dr

2v
95% (48 h)
>99% ee (major)
>99% ee (minor)
1.3/1 dr

2w
86% (48 h)
>99% ee (major)
>99% ee (minor)
1.2/1 dr

2x
0% (48 h)

[a] Reaction conditions: **1** (0.1 mmol unless otherwise notified), CoSO₄·7H₂O (10 mol%), Mn(OAc)₃·2H₂O (1 equiv.), PivONa·2H₂O (2 equiv.), **L1** (20 mol%), ⁿPrOH (0.05 M), air, 50°C, reacted for 24 h unless notified.
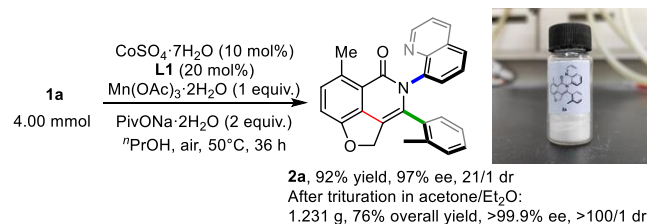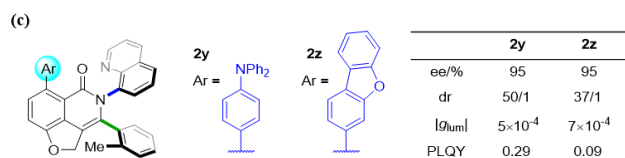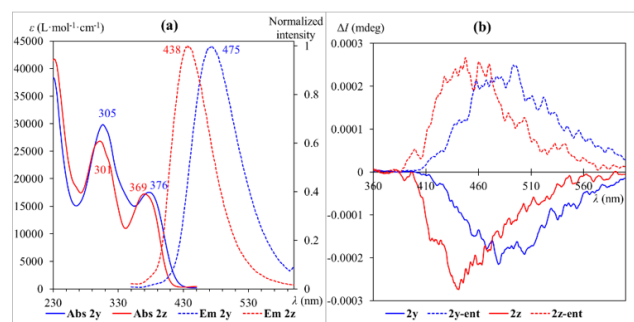
4

1a
4.00 mmol

CoSO₄·7H₂O (10 mol%)
L1 (20 mol%)
Mn(OAc)₃·2H₂O (1 equiv.)
PivONa·2H₂O (2 equiv.)
ⁿPrOH, air, 50°C, 36 h

2a, 92% yield, 97% ee, 21/1 dr
After trituration in acetone/Et₂O:
1.231 g, 76% overall yield, >99.9% ee, >100/1 dr

Scheme 1. Gram scale synthesis of **2a**.

Figure 3. (a) Absorption and emission spectra of **2y** and **2z** (maxima indicated); (b) CPL spectra of **2y**, **2y-ent**, **2z** and **2z-ent**; (c) Structure, optical purity, dissymmetry factor and PLQY of **2y** and **2z**.

	2y	2z
ee/%	95	95
dr	50/1	37/1
$|g_{lum}|$	5×10^{-4}	7×10^{-4}
PLQY	0.29	0.09

Investigations on Atropisomerization Mechanism. To gain more mechanistic insights into the atropisomerization of the products, we next performed density functional theory (DFT) calculations to investigate how each axis rotates and whether the concerted rotation pathway exists or not. As shown in Figure 4, from **2a-Conf-1**, the C–C axis rotates through **2a-TS12** to give the diastereomer **2a-Conf-2**, which requires a free energy barrier of 127.9 kJ/mol. The more facile C–N axis rotation in **2a-Conf-2** via **2a-TS23** leads to **2a-Conf-3**, with a lower free energy barrier of 118.5 kJ/mol. Then the C–C axis rotation in **2a-Conf-3** takes place through **2a-TS34**, leading to **2a-Conf-4**. Eventually, a C–N axis rotation via **2a-TS41** transfers **2a-Conf-4** to **2a-Conf-1**, thus completing the conformation inversion of **2a**.

In addition, concerning the steric effect between two vicinal axes, we initially hypothesized a concerted two-axis rotation pathway between two enantiomers (i.e. **2a-Conf-1** to **2a-Conf-3**, **2a-Conf-2** to **2a-Conf-4**).[5b,18] Investigation on the free energy surface of conformation inversion indicates that this assumed concerted rotation pathway does not exist (see Figure S5 of the Supporting Information for details). Instead, we have located a stepwise inversion pathway between **2a-Conf-2** and **2a-Conf-4**, which is unlikely because of a relatively high overall activation free energy of 152.0 kJ/mol (Figure 4, dashed curves).
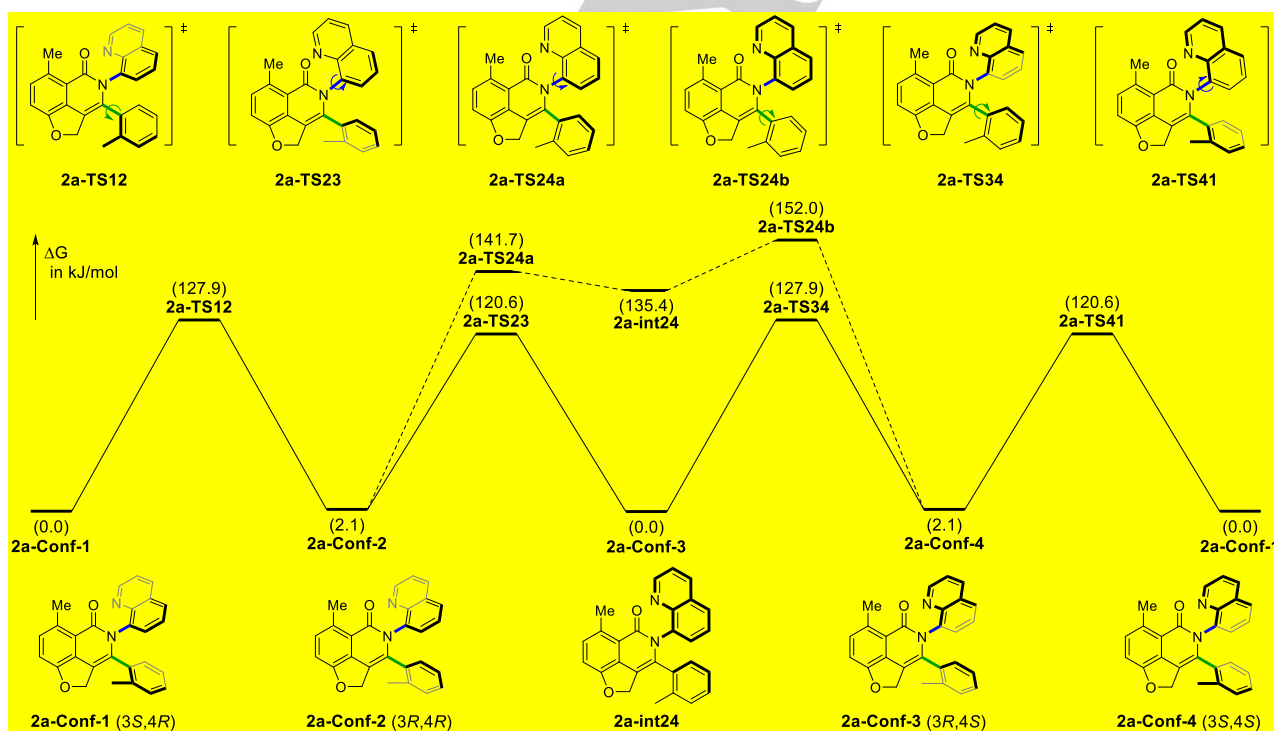
Figure 4. Free energy profile of conformation inversion pathways of **2a**. Solid curve: single-axis rotation pathways. Dashed curve: the stepwise, high-energy but straight inversion pathway between **2a-Conf-2** and **2a-Conf-4**. All energies were calculated at the B3LYP-D3(BJ)/6-311+G(d, p)-SMD(*o*-xylene)// B3LYP-D3(BJ)/6-31G(d)-SMD(*o*-xylene) level of theory.

Next, we considered the atropisomerization of **2c**, **2d**, **2e**, and **2f**. As shown in Figure 5a, the diastereomers of **2a** and **2c** are similar in a low free energy difference of 2.1 kJ/mol and 2.2 kJ/mol, respectively. In contrast, the diastereomers of **2e** and **2d** have a more significant free energy difference of 10.0 kJ/mol and 13.7 kJ/mol, respectively. The C–C single-axis rotation barrier is consistent with the steric hindrance of *ortho*-substituent in the phenyl group (R¹). The products (**2a** and **2d**) with less steric hindered methyl and chloro groups, possess a lower inversion free energy barrier of 10.0 kJ/mol and 13.7 kJ/mol, respectively (Figure 5a, entry 1 and 3), and for products bearing larger isopropyl and trifluoromethyl groups (**2c** and **2e**), this inversion

5

barrier increases to 144.1 kJ/mol and 141.0 kJ/mol, respectively (entry 2 and 4). In addition, **2f** with only one chiral C–N axis has a rotation free energy barrier of 115.6 kJ/mol, consistent with the experimentally measured free energy barrier of 113.9 kJ/mol (Figure 5b). Products **2f**, **2a**, **2d**, **2c** and **2e**, bearing increasingly larger *ortho*-substituents,[19] show a rising trend of the C–N axis rotation barriers, indicating that the steric effect of the C–C axis can affect the atropostability of the vicinal C–N axis, as we have expected.

2a, R¹ = Me
2c, R¹ = *i*Pr
2d, R¹ = Cl
2e, R¹ = CF₃

ΔG(**Conf-1/3**) = 0.0 kJ/mol

Entry	Product	ΔG(Conf-2/4) (kJ/mol)	ΔG‡cal.(C-C axis) (kJ/mol)	ΔG‡cal.(C-N axis) (kJ/mol)
1	**2a**	2.1	127.9	120.6
2	**2c**	2.2	144.1	122.5
3	**2d**	10.0	128.3	122.4
4	**2e**	13.7	141.0	124.8

ΔG‡cal. = 115.6 kJ/mol
ΔG‡exp. = 113.9 kJ/mol

PMP = *p*-methoxyphenyl
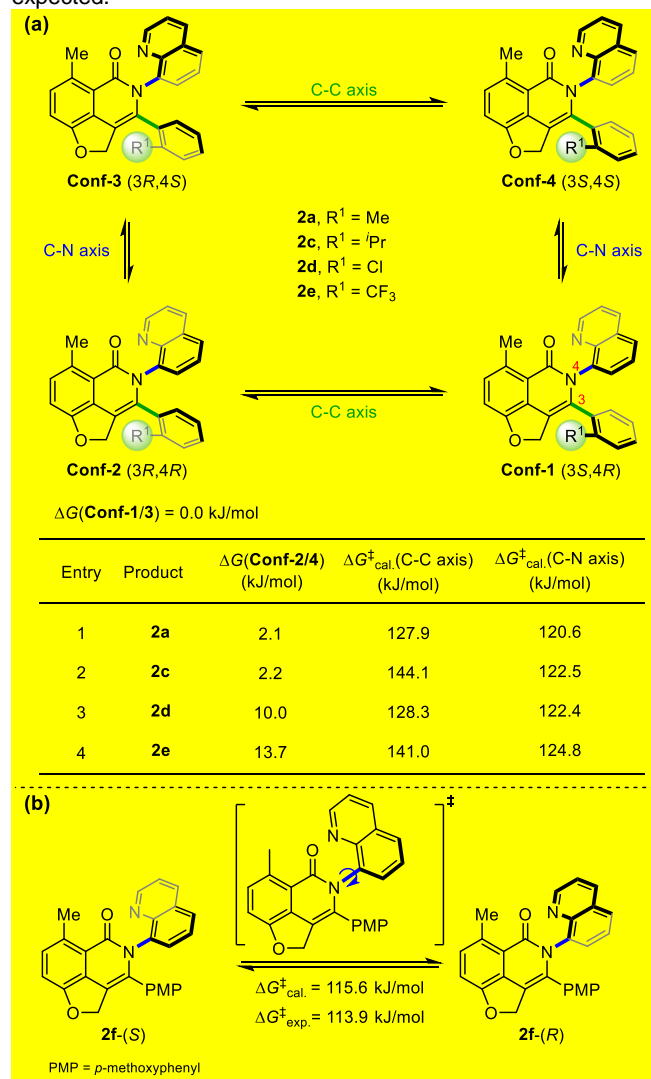
Figure 5. a) Atropisomerization of **2a**, **2c**, **2d**, and **2e**. All energies were calculated at the B3LYP-D3(BJ)/6-311+G(d, p)-SMD(*o*-xylene)//B3LYP-D3(BJ)/6-31G(d)-SMD(*o*-xylene) level of theory. b) Conformation inversion of **2f**. All energies were calculated at the B3LYP-D3(BJ)/6-311+G(d, p)-SMD(2-propanol)//B3LYP-D3(BJ)/6-31G(d)-SMD(2-propanol) level of theory.

Conclusion

In summary, we have presented a cobalt-catalyzed C–H annulation by atroposelective intramolecular alkyne insertion for the single-step construction of atropisomers with vicinal C–C and C–N chiral diaxes. This protocol provided over 20 examples of products possessing unique structures with two chiral events moderately to well stereocontrolled. Products modified with large conjugated aryls exhibit noticeable CPL-activities, being candidate materials for potential CPL applications. Atropisomerization experiments and DFT calculations revealed that the rotational barriers of the C–N axes were of similar magnitude and effected by the steric bulkiness of the ortho-

substituents of C–C axis, whose rotation barrier varied noticeably with the steric bulkiness of the ortho-substituents. The DFT investigation on the free energy surface of atropisomerization excluded the possibility of concerted rotation of two axes.

[1] (a) C. Zheng, S.-L. You, *RSC Adv.* **2014**, *4*, 6173-6214. (b) C. G. Newton, S.-G. Wang, C. C. Oliveira, N. Cramer, *Chem. Rev.* **2017**, *117*, 8908–8976. c) T. G. Saint-Denis, R.-Y. Zhu, G. Chen, Q.-F. Wu, J.-Q. Yu, *Science* **2018**, *359*, eaao4798. (d) J. Loup, U. Dhawa, F. Pesciaioli, J. Wencel-Delord, L. Ackermann, *Angew. Chem. Int. Ed.* **2019**, *58*, 12803–12818. (e) T. Yoshino, S. Satake, S. Matsunaga, *Chem. - Eur. J.* **2020**, *26*, 7346–7357. (f) T. Achar, S. Maiti, S. Jana, D. Maiti, *ACS Catal.* **2020**, *10*, 13748–13793. (g) Q. Zhang, B.-F. Shi, *Acc. Chem. Res.* **2021**, *54*, 2750–2763.

[2] (a) C.-X. Liu, W.-W. Zhang, S.-Y. Yin, Q. Gu, S.-L. You, *J. Am. Chem. Soc.* **2021**, *143*, 14025–14040. (b) J. K. Cheng, S.-H. Xiang, S. Li, L. Ye, B. Tan, *Chem. Rev.* **2021**, *121*, 4805–4902. (c) J. Wencel-Delord, F. Colobert, *SynOpen* **2020**, *04*, 107–115. (d) G. Liao, T. Zhou, Q.-J. Yao, B.-F. Shi, *Chem. Commun.* **2019**, *55*, 8514–8523. (e) G. Shan, J. Flegel, H. Li, C. Merten, S. Ziegler, A. P. Antonchick, H. Waldmann, *Angew. Chem. Int. Ed.* **2018**, *57*, 14250–14254.

[3] For selected reviews, see: (a) X. Bao, J. Rodriguez, D. Bonne, *Angew. Chem. Int. Ed.* **2020**, *59*, 12623–12634. (b) T. A. Schmidt, C. Sparr, *Acc. Chem. Res.* **2021**, *54*, 2764–2774.

[4] (a) L. Jin, P. Zhang, Y. Li, X. Yu, B.-F. Shi, *J. Am. Chem. Soc.* **2021**, *143*, 12335–12344. (b) G. Liao, T. Zhang, L. Jin, B.-J. Wang, C.-K. Xu, Y. Lan, Y. Zhao, B.-F. Shi, *Angew. Chem. Int. Ed.* **2022**, e202115221. (c) Z.-S. Liu, P.-P. Xie, Y. Hua, C. Wu, Y. Ma, J. Chen, H.-G. Cheng, X. Hong, Q. Zhou, *Chem.* **2021**, *7*, 1917–1932.

[5] (a) T. Shibata, K. Tsuchikama M. Otsuka, *Tetrahedron: Asymmetry* **2006**, *17*, 614–619. (b) K. T. Barrett, A. J. Metrano, P. R. Rablen, S. J. Miller, *Nature* **2014**, *509*, 71–75. (c) D. Lotter, M. Neuburger, M. Rickhaus, D. Häussinger, C. Sparr, *Angew. Chem., Int. Ed.* **2016**, *55*, 2920−2923. (d) D. Lotter, A. Castrogiovanni, M. Neuburger, C. Sparr, *ACS Cent. Sci.* **2018**, *4*, 656–660. (e) Y. Tan, S. Jia, F. Hu, Y. Liu, L. Peng, D. Li, H. Yan, *J. Am. Chem. Soc.* **2018**, *140*, 16893–16898. (f) Y.-L. Hu, Z. Wang, H.

6

Yang, J. Chen, Z.-B. Wu, Y. Lei, L. Zhou, *Chem. Sci.* **2019**, *10*, 6777–6784.

[6] (a) Q. Dherbassy, J.-P. Djukic, J. Wencel-Delord, F. Colobert, *Angew. Chem. Int. Ed.* **2018**, *57*, 4668–4672. (b) Q. Dherbassy, J. Wencel-Delord, F. Colobert, *Tetrahedron* **2018**, *74*, 6205–6212.

[7] Q. Gao, C. Wu, S. Deng, L. Li, Z.-S. Liu, Y. Hua, J. Ye, C. Liu, H.-G. Cheng, H. Cong, Y. Jiao, Q. Zhou, *J. Am. Chem. Soc.* **2021**, *143*, 7253−7260.

[8] (a) Q.-J. Yao, S. Zhang, B.-B. Zhan, B.-F. Shi, *Angew. Chem. Int. Ed.* **2017**, *56*, 6617–6621. (b) G. Liao, Q.-J. Yao, Z.-Z. Zhang, Y.-J. Wu, D.-Y. Huang, B.-F. Shi, *Angew. Chem. Int. Ed.* **2018**, *57*, 3661–3665. (c) J. Luo, T. Zhang, L. Wang, G. Liao, Q.-J. Yao, Y.-J. Wu, B.-B. Zhan, Y. Lan, X.-F. Lin, B.-F. Shi, *Angew. Chem. Int. Ed.* **2019**, *58*, 6708–6712. (d) L. Jin, Q.-J. Yao, P.-P. Xie, Y. Li, B.-B. Zhan, Y.-Q. Han, X. Hong, B.-F. Shi, *Chem* **2020**, *6*, 497–511. (e) H. Song, Y. Li, Q.-J. Yao, L. Jin, L. Liu, Y.-H. Liu, B.-F. Shi, *Angew. Chem. Int. Ed.* **2020**, *59*, 6576–6580. (f) Q.-J. Yao, P.-P. Xie, Y.-J. Wu, Y.-L. Feng, M.-Y. Teng, X. Hong, B.-F. Shi, *J. Am. Chem. Soc.* **2020**, *142*, 18266–18276.

[9] V. G. Zaitsev, D. Shabashov, O. Daugulis, *J. Am. Chem. Soc.* **2005**, *127*, 13154–13155.

[10] (a) T. Yoshino, S. Matsunaga, *Adv. Synth. Catal.* **2017**, *359*, 1245–1262. (b) J. Park, S. Chang, *Chem. Asian J.* **2018**, *13*, 1089–1102. (c) S. Prakash, R. Kuppusamy, C.-H. Cheng, *ChemCatChem* **2018**, *10*, 683–705. (d) R.–H. Mei, U. Dhawa, R. C. Samanta, W.-B. Ma, J. Wencel-Delord, L. Ackermann, *ChemSusChem* **2020**, *13*, 3306–3356.

[11] B. Ye, P. A. Donets, N. Cramer, *Angew. Chem. Int. Ed.* **2014**, *53*, 507–511.

[12] Q.-J. Yao, J.-H. Chen, H. Song, F.-R. Huang, B.-F. Shi, *Angew. Chem. Int. Ed.* **2022**, e202202892.

[13] (a) I. Takahashi, Y. Suzuki, O. *Org. Prep. Proced. Int.* **2014**, *46*, 1-23. (b) O. Kitagawa, *Acc. Chem. Res.* **2021**, *54*, 719–730. (c) Y.-J. Wu, G. Liao, B.-F. Shi, *Green Synth. Catal.* **2022**, *3, 117–136.*

[14] For examples of Co(III)-catalyzed enantioselective C-H activation, see: (a) F. Pesciaioli, U. Dhawa, J. C. A. Oliveira, R. Yin, M. John, L. Ackermann, *Angew. Chem. Int. Ed.* **2018**, *57*, 15425–15429. (b) S. Fukagawa, Y. Kato, R. Tanaka, M. Kojima, T. Yoshino, S. Matsunaga, *Angew. Chem., Int. Ed.* **2019**, *58*, 1153–1157. (c) D. Sekine, K. Ikeda, S. Fukagawa, M. Kojima, T. Yoshino, S. Matsunaga, *Organometallics* **2019**, *38*, 3921–3926. (d) Y.-H. Liu, P.-X. Li, Q.-J. Yao, Z.-Z. Zhang, D.-Y. Huang, M.-D. Le, H. Song, L. Liu, B.-F. Shi, *Org. Lett.* **2019**, *21*, 1895–1899. (e) Y.-H. Liu, P.-P. Xie, L. Liu, J. Fan, Z.-Z. Zhang, X. Hong, B.-F. Shi, *J. Am. Chem. Soc.* **2021**, *143*, 19112–19120. (f) W.-K. Yuan, B.-F. Shi, *Angew. Chem. Int. Ed.* **2021**, *60*, 23187–23192. (g) K. Ozols, Y.-S. Jang, N. Cramer, *J. Am. Chem. Soc.* **2019**, *141*, 5675–5680. (h) K. Ozols, S. Onodera, Ł. Woźniak, N. Cramer, *Angew. Chem., Int. Ed.* **2021**, *60*, 655–659. (i) A. G. Herriz, N. Cramer, *ACS Catal.* **2021**, *11*, 11938–11944.

[15] (a) L. Grigorjeva, O. Daugulis, *Angew. Chem. Int. Ed.* **2014**, *53*, 10209–10212. (b) L. Grigorjeva, O. Daugulis, *Org. Lett.* **2014**, *16*, 4684–4687.

[16] Deposition Numbers 2132392, 2132394, 2132395, and 2132393 contain the supplementary crystallographic data for this paper. These data are provided free of charge by the joint Cambridge Crystallographic Data Centre and Fachinformationszentrum Karlsruhe Access Structures service.

[17] (a) E. M. Sánchez-Carnerero, A. R. Agarrabeitia, F. Moreno, B. L. Maroto, G. Muller, M. J. Ortiz S. de la Moya, *Chem. Eur. J.* **2015**, *21*, 13488–13500. (b) M. Li, W.-B. Lin, L. Fang, C.-F. Chen, *Acta Chim. Sinica* **2017**, *75*, 1150–1163.

[18] (a) A. Ahmed, R. A. Bragg, J. Clayden, L. W. Lai, C. McCarthy, J. H. Pink, N. Westlund S. A. Yasin, *Tetrahedron* **1998**, *54*, 13277–13294. (b) H. Iwamura, K. Mislow, *Acc. Chem. Res.* **1988**, *21*, 175–182.

[19] V. Belot, D. Farran, M. Jean, M. Albalat, N. Vanthuyne, C. Roussel, *J. Org. Chem.* **2017**, *82*, 10188−10200.

7

Entry for the Table of Contents
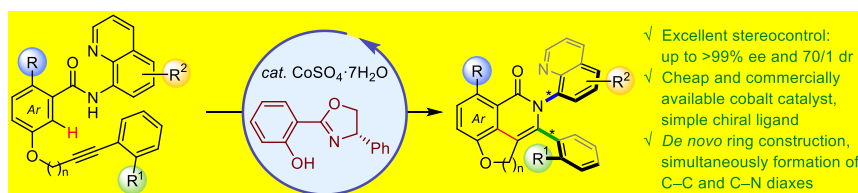
A single-step construction of atropisomers with vicinal C–C and C–N chiral diaxes by cyclopentadiene (Cp)-free cobalt-catalyzed intramolecular atroposelective C–H annulation with decent stereocontrols (up to >99% ee and 70/1 dr) was reported. Atropisomerization experiments and DFT calculations are done to study the rotational barriers and pathways of the diaxes.

Institute and/or researcher Twitter usernames: ((bfshi))